Global Mapping of Equilibrium and Transition Structures on Potential Energy Surfaces by the Scaled Hypersphere Search Method: Applications to ab Initio Surfaces of Formaldehyde and Propyne Molecules

Satoshi Maeda and Koichi Ohno*

Department of Chemistry, Graduate School of Science, Tohoku University, Aramaki, Aoba-ku, Sendai 980-8578, Japan

Received: March 14, 2005; In Final Form: April 23, 2005

Technical details of a new global mapping technique for finding equilibrium (EQ) and transition structures (TS) on potential energy surfaces (PES), the scaled hypersphere search (SHS) method (Ohno, K.; Maeda, S. *Chem. Phys. Lett.* **2004**, *384*, 277), are presented. On the basis of a simple principle that reaction pathways are found as anharmonic downward distortions of PES around an EQ point, the reaction pathways can be obtained as energy minima on the scaled hypersphere surface, which would have a constant energy when the potentials are harmonic. Connections of SHS paths between each EQ are very similar to corresponding intrinsic reaction coordinate (IRC) connections. The energy maximum along the SHS path reaches a region in close proximity to the TS of the reaction pathway, and the subsequent geometry optimization from the SHS maximum structure easily converges to the TS. The SHS method, using the one-after-another algorithm connecting EQ and TS, considerably reduces the multidimensional space to be searched to certain limited regions around the pathways connecting each EQ with the neighboring TS. Applications of the SHS method have been made to ab initio surfaces of formaldehyde and propyne molecules to obtain systematically five EQ and nine TS for formaldehyde and seven EQ and 32 TS for propyne.

I. Introduction

Potential energy surfaces (PES) have great significance in connection with molecular structures, molecular properties, and chemical reactions; thus, exploring the global topology of PES is very important in physical chemistry.[1] However, it is impossible to examine all points on multidimensional PES described by $3N - 6$ degrees of vibrational freedom for an N-atom system. The topology of PES can be overviewed by searching for connections between equilibrium structures (EQ) and transition structures (TS) via an intrinsic reaction coordinate (IRC),[2] and their energy, structure, and curvature around them enable us to make discussions and analyses of chemical reactions. Reaction rate constants can be calculated by the transition state theory (TST)[3−5] followed by multiwell master equation approaches[6−8] even when competitive reactions were concerned. In molecular dynamics calculations, an IRC network is also important to make efficient sampling of reference points for construction of global PES by interpolation techniques such as the modified Shepard interpolation technique.[9−11] On the other hand, accurate quantum chemical calculations enable us to predict gas-phase reactions by searching for EQ and TS on PES, and there are many theoretical reports concerning chemical reactions in interstellar space,[12−17] planet atmosphere,[18−22] and combustion processes.[23−25] Thus, it is important to develop a technique that enables us to make efficient global mapping of PES for the purpose of statistical or dynamical analyses and prediction of chemical reactions.

EQ and TS are energy minima and first-order saddle points on PES, respectively, and then the above problem corresponds to searching for points satisfying these mathematical conditions on multivariable functions. Westerberg and Floudas developed the α-BB method as a mathematical procedure that examines the mathematical condition for the whole surface by appropriate grid separations.[26] Although the α-BB method is deterministic for obtaining all EQ and TS within its grid accuracy, applications of the α-BB method toward systems described by all degrees of freedom are limited only for very simple three-atom systems.[26] Since the configuration space of bond rearrangement and the dissociation part of PES is very extensive or infinite, the deterministic approach is useful only for conformation sampling of amino acids or proteins described only by their internal rotation angles with a finite length of 2π radian. It is still very difficult or impossible to examine the mathematical condition for whole infinitely spreading $3N - 6$ dimensional space with a fine-tooth comb, even in very small four- or five-atom systems.

In general, EQ and TS are searched by geometry optimization techniques such as rational function optimization (RFO)[27] or the geometry direct inversion in iterative subspace (GDIIS)[28] method. Although these techniques can reach the nearest stationary point from the initially assumed geometry, the obtained structure strongly depends on the choice of initial guess. These methods can search for EQ and TS if its crude estimation can previously be made by chemical intuition; otherwise, any separate use of these techniques requires many trial-and-error procedures starting from many initial structures. For the purpose of analyses of multichannel and multiwell reactions or predictions of unknown chemical reactions, we need to develop a technique that does not require any initial guesses.

There are many techniques searching for EQ and TS by walking on PES starting from a stationary point toward another stationary point. One of the most accepted ones is the eigen-

* Corresponding author. E-mail address: ohnok@qpcrkk.chem.tohoku.ac.jp.

10.1021/jp0513162 CCC: $30.25
Published on Web 06/07/2005

vector following (EF) technique.[29−34] The EF can locate a stationary point by walking toward an eigenvector direction of normal-mode analyses if it exists in the chosen eigenvector direction. In application of the EF to Lenard-Jones Ar clusters, Tsai and Jordan demonstrated global mapping of PES by walking toward all $2(3N - 6)$ eigenvector directions (forward and reverse directions of all eigenvectors of N atomic system) starting from EQ and TS obtained in the prosess.[35] Another surface-walking approach, gradient extremal following (GEF),[29,36−44] has the excellent feature of following uphill and downhill valleys on PES, and it has been considered as the full-CI of PES analyses,[45] though there is an example where an EQ is isolated in GEF path connections.[43] Bondensgård and Jensen applied the GEF to the ab initio PES of formaldehyde[44] and presented the first systematic global analysis of ab initio PES for more than three-atom system. After that, the new global analysis of the PES of the formaldehyde molecule was made by application of reduced gradient following (RGF)[46−51] developed by Quapp et al.,[46] and some EQ corresponding to weekly bound dissociated structures were newly reported. It should be noted that $2(3N - 6)$ pathways should be treated from all stationary points in these three surface walking approaches if one aims at fully global analyses. Although some of these pathways reach to EQ or TS, many others should wander around useless high energy parts of PES strongly deviated from IRC connections. The wandering feature of these methods can be seen in behavior of these walking approaches on two-dimensional model potentials,[35,43,46] and applications of GEF and RGF to six-dimensional ab initio PES demonstrated the much too complicated connections of their pathways.[44,46] Thus, further applications of these approaches toward more complicated systems are difficult without any modifications or simplifications.

In many cases, the number of searching directions is considerably reduced by selecting certain ones among the $2(3N - 6)$ eigenvector directions, since the number of eigenvector directions and starting stationary points increase extremely rapidly. In the activation relaxation technique (ART) of Barkema and Mousseau,[52,53] the lower energy EQ was searched starting from randomly packed amorphous structures with activations toward a randomly chosen direction followed by judgment whether newly found EQ should be accepted or not according to the Metropolis Monte Carlo acceptance criterion. Wales et al. developed the n_{ev}-complete method, which chooses n_{ev} eigenvector directions with the lowest n_{ev} eigenvalues as searching directions in EF procedures.[54,55] Laio and Parrinello (LP) proposed the biasing technique of PES by use of suitable Gaussian functions,[56−58] and the LP method accelerates to reach a new potential well by escaping the deep well in which it is currently trapped in molecular dynamics (MD) simulations. The ART, n_{ev}-complete, and LP methods are very efficient and useful for statistical sampling of the lower energy part of PES, because of the lower energy seeking nature of their basis, i.e., Monte Carlo criteria, choosing the softest n_{ev} eigenvector directions, and MD simulation.

However, the higher energy part of PES is also important in chemistry. For example, high-temperature combustion processes, including many radical reactions, yield extensive bond rearrangement and dissociation reactions. The photoexcitation−relaxation process sometimes falls down on a very high energy part of the ground state PES, and a high barrier can easily be overcome in such highly excited molecules. Furthermore, radical reactions and ion−molecule reactions are important for predicting chemical reactions in the atmosphere or interstellar spaces, because a barrierless reaction only can proceed in very cold interstellar molecular clouds. In such cases, the product structure is previously known from spectroscopic analyses of their rotational or vibration radiations; thus, one has to make extensive uphill walking starting from the structure toward reasonable radical dissociation channels (lying on ca. 100 kcal/mol area of PES).

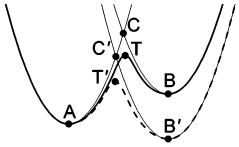

Figure 1. Schematic illustration of reaction potentials around two equilibrium positions, A and B(B′). The crossing points C and C′ for the harmonic potentials are closely related to the transition states T and T′.

For these purposes, lower energy seeking approaches such as Monte Carlo or MD simulation are not suitable for choosing walking directions on PES. Since in many cases EQ is connected with some TS via reaction paths, an algorithm following reaction paths to search EQ and TS one after another is highly promising. The fundamental problem is how to seek the reaction path direction at a starting EQ. This seems to be very difficult, because IRC can only be defined by integrating the steepest descent path starting from TS. However, PES of chemical systems are essentially governed by quantum chemical characteristics. The frontier orbital theory[59,60] is a typical example in which electronic state properties can be used to deduce the most likely TS of chemical reactions. Also, the heights or the locations of TS have been deduced from intersections of harmonic potential curves located at geometries of the reactant and the product, as indicated schematically in Figure 1; the positions and the heights of TS (T and T′) are in good accordance with those of crossing points of harmonic potentials (C and C′), which depend essentially on the relative heights of the equilibrium structures B and B′ with respect to A. These characteristics have been used in the Marcus equation;[61] Bell, Evans, and Polanyi principle;[4,62] and the Hammond postulate.[63] More quantitatively, the concept of Figure 1 was used to estimate a TS between two known minima.[64−66] According to these traditional methods concerning the chemical nature of PES, we arrive at an uphill walk method following reaction paths from EQ to TS or DC based on the scaled hypersphere search algorithm.[67]

The scaled hypersphere search (SHS) method can search for reaction channels by walking on PES guided by anharmonic downward distortions from the second-order surface expanded at the starting EQ, and its walk along the SHS path leads to another potential well or dissociation channels.[67] In some typical cases, its walk was demonstrated to pass thorough nearby TS of corresponding reactions,[67,68] and then geometry optimizations starting from the energy maxima of SHS paths can locate related TS. Thus, we can make global mapping of EQ and TS by following SHS paths starting from all EQ obtained by the process. We already reported a new synthetic reaction route of glycine molecule from three simple species (CO_2, NH_3, CH_2) by applications of the SHS method.[69,70] Furthermore, we presented an approach by the SHS method for finding TS between a reactant and a product and demonstrated that the SHS method can make a highly accurate estimation of TS.[68]

In this paper, we describe the procedure of global mapping of EQ and TS on PES by the SHS method. We applied the SHS method to the four-atom molecule formaldehyde described by the B3LYP/6-31G level of theory and also had detailed

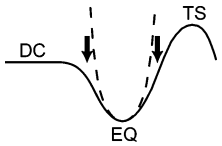

Figure 2. Schematic illustration of reaction pathways around an equilibrium structure EQ leading to the transition state TS and the dissociation channel DC with respect to the harmonic potential shown by a dashed curve, from which reaction potentials undergo anharmonic downward distortions indicated by arrows.

discussions about the character of the SHS paths and the efficiency of the SHS method. We present another example of the application of the SHS method to the seven-atom molecule propyne described by the HF/6-31G level of theory. Obtained structures and IRC connections by the SHS method were refined by the higher B3LYP/6-311++G(d,p) level of theory using structures of low level calculations as initial guesses, and then one-point energy calculations were made by the CCSD(T)/cc-pVTZ level of theory at optimized structures by B3LYP/6-311++G(d,p). Finally, five EQ and nine TS for formaldehyde and seven EQ and 32 TS for propyne were obtained on B3LYP/6-311++G(d,p) surfaces.

II. Method

A. The Scaled Hypersphere Search Method. As illustrated in Figure 1, TS (T and T′) are more or less related to crossing points C and C′, which are linked with the relevant EQ (A and B, B′) on the PES of chemical systems. It should be noted that the real PES around the EQ undergoes anharmonic downward distortions from the harmonic potentials because of the continuous connections among the EQ and the TS. Typical reaction paths always change their curvatures from concave to convex on going to TS or DC, as can be seen in Figure 2. This indicates that slopes should always decline their inclinations because of the energy-lowering interactions leading to TS or DC. When one starts from an EQ of the PES, an indication of a reaction path will appear as an energy lowering with respect to its neighbors. Thus, one may expect that the reaction pathways can be found as downward distortions on the potential surface. An efficient algorithm finding downward distortions around an EQ can be obtained by comparison of the real potential energies on a closed surface defined by a given reference harmonic energy.

At an EQ for a given chemical composition, normal coordinates should be determined at first. Around the EQ, PES can be expanded in terms of the normal coordinates Q_i with respective eigenvalues λ_i. For systematic treatments, the scaled normal coordinates defined by $q_i = \lambda_i^{1/2} Q_i$ are suitable, since this representation transforms a reference hypersurface into a hypersphere surface on which every point should have the same energy for the reference harmonic potentials. This scaled hypersphere representation makes it easy to find anharmonic downward distortions. The use of the hypersphere has a significant advantage that all directions can be treated equivalently and thoroughly. The treatment with the hypersphere is very important, since reaction paths are not always along particular normal mode directions but possibly along intermediate directions corresponding to mixtures of several normal coordinates.

Distinct downward deformations of PES can be detected as minima on the scaled hypersphere with a center at the EQ. Each energy minimum on the hypersphere indicates an individual downward distortion of the potential. Hence, pathways to TS or DC around EQ may be traced via energy minima on the scaled hypersphere surface. Using several sizes of hypersphere, we can obtain a series of points for the pathways around the EQ. These paths can be denoted as scaled hypersphere search (SHS) paths. If the magnitude of the gradient at each minimum on the hypersphere becomes smaller than a threshold value, further tests are made to confirm the type of stationary point. An indication of a TS region can be obtained from the gradient of the SHS path point. The location of each TS can be determined precisely by an application of a conventional technique in the TS region.[27,28] Asymptotic behavior separating a fragment from the remaining part indicates a DC. Once entered into another basin after passing through the TS region, downhill walking along the steepest descent path[71−79] allows us to find a new EQ. These procedures are made for all obtained EQ, and then a global survey of the PES for a given chemical composition can be achieved (see section II.D for details on the algorithm).

There are some uphill walking techniques that use energy minimization on the nonscaled hypersphere surface.[72,80,81] Although the mathematical procedure of the present SHS method is very similar to those of other techniques, the chemical meaning of the SHS path is completely different from their uphill-valley-following concept. The idea of the present method is to follow the downward distortion of the PES from the harmonic surface, as discussed above, and then the SHS path sometimes has different characteristics from the uphill valley of the PES.

B. Discovery Technique for Nearly Overlapped Pathways. Although a downward distortion leading to TS or DC can be obtained as a local minimum on the hypersphere surface, the situation will become complicated if several pathways are nearly overlapped around an EQ. Energy lowering of neighboring pathways may possibly overlap on the hypersphere, and then downward distortions caused by relatively weak interactions should be obscured or hidden by deeper distortions due to much stronger interactions. In spectroscopic analyses, overlapped signals are conventionally separated by suitable peak-fitting or deconvolution techniques. Thus, overlapped dents on the hypersphere surface can also be decomposed into individual components.

There are some techniques for fitting PES by use of some kind of functions. The modified Shepard interpolation technique by Ichitwan and Collins[9] uses weighted averages of locally expanded second-order functions.[9−11] There is another approach by Laio and Parrinello using Gaussian functions for fitting the PES,[56] and this approach was used for escaping from free-energy wells as fast as possible in molecular dynamics simulations.[56−58] We used cosine functions for fitting energy functions on scaled hypersphere surfaces, on the basis of the third-order fitting of PES around an EQ.

We introduce a peak-fitting technique on the hypersphere surface. The degree of freedom of the scaled normal coordinates q_1, q_2, ..., q_f in the system is denoted as f, which is related with the number of atoms N in the system ($f = 3N - 6$ for a nonlinear system). By use of the scaled normal coordinate, the potential energy at a point indicated by vector $\mathbf{s}$ can be expanded as eq 1 with third-order approximations around the EQ.

$$E(\mathbf{s}) = \frac{1}{2}|\mathbf{s}|^2 + \frac{1}{6}F|\mathbf{s}|^3 \qquad (1)$$

Here, energy at the EQ was set to be zero, and the parameter F is corresponding to the third-order derivative along $\mathbf{s}$ (the second-order derivative equal to unity in the scaled coordinate). An approximate energy function can be given as eq 2, by

assuming third-order derivative tensor components along any other directions and coupling terms of them to be zero,

$$E(\mathbf{q}) = \epsilon + \frac{1}{6}F|\mathbf{q}\cdot\mathbf{t}|^3 = \epsilon + \frac{1}{6}F|\mathbf{q}|^3\cos^3\theta \qquad (2)$$

where **q** is a vector indicating an arbitrary point on the hypersphere, ***t*** is the unit vector directing **s** (i.e. $\mathbf{t} = \mathbf{s}/|\mathbf{s}|$), ϵ is corresponding to the harmonic energy, and θ is the angle between **s** and **q**. On the basis of the approximation leading to eq 2, a shape function $G(\mathbf{q})$ for fitting each local downward minimum yielding the respective SHS path at $\mathbf{s}(q_1, q_2, ..., q_f)$ should be written by use of a cosine function.

$$G(\mathbf{q}) = A\cos^3\theta \quad (\theta \le \pi/2) \qquad (3)$$

Here, A is the depth parameter of the corresponding minimum and can simply be determined as $A = \epsilon - E(\mathbf{s})$. Although the shape function $G(\mathbf{q})$ in eq 3 is obtained according to eq 1 truncated at third order, parameter A ($=1/6F|\mathbf{q}|^3$) is including higher order terms effectively, since A is determined by use of the exact energy value $E(\mathbf{s})$ at the current point **s**. Since the function value, the first derivative, and the second derivative of $G(\mathbf{q})$ with respect to θ are zero at $\theta = \pi/2$, $G(\mathbf{q})$ is confirmed to be continuous up to the second order on the hypersphere if it is truncated at $\theta = \pi/2$.

After having obtained a set of shape functions for n individual downward minima, a modified surface, where the initial n minima are eliminated, can be deduced as $E'(\mathbf{q}) = E(\mathbf{q}) + \sum_{i=1}^{n} G_i(\mathbf{q})$. This modified surface $E'(\mathbf{q})$ is considered to contain hidden downward minima if they exist. Thus, we should search again local downward minima on this modified hypersphere surface. After having found the new n' downward minima, the above treatments should be repeated to seek hidden minima, until no hidden minima are discovered.

The present cosine-expansion treatments may yield some artificial dents and lead to some additional SHS paths. To avoid such problems, a criterion to discard unwanted minima is introduced. The energy $E'(\mathbf{q})$ at a hidden minimum is compared with the depth parameter A_i of fitting function centered at the ith previous minimum, giving the largest contribution at the position of the hidden minimum. When the ratio of the downward distortions, $d = (\epsilon - E'(\mathbf{q}))/A_i$, is smaller than a certain threshold value, the hidden minimum is discarded. In some test calculations, $d = 0.2$ was dangerous because some important reaction paths were overlooked, and $d = 0.05$ yielded many artificial dents. A threshold value of $d = 0.1$ was found to be satisfactory in the present study and was used in calculations of both formaldehyde and propyne molecules.

C. Iterative Optimization−Elimination (IOE) Technique for Finding All SHS Paths. The present SHS method requires an efficient technique to find out all SHS paths around an arbitrary EQ. In view of applications to ab initio PES, computational demands should be reduced to be as small as possible, since the number of geometries for ab initio calculations may become too large to be handled for the multidimensional PES. Thus, efficient techniques should be developed to find all SHS paths for large systems.

For this purpose, we have developed an iterative optimization−elimination (IOE) technique for finding all SHS paths. This method is based on the technique for discovering overlapped downward distortions described in detail in section II.B and also on the geometry optimization and energy gradient techniques in conventional quantum chemical packages. This method is somewhat related with biased approaches for finding global minima,[82,83] efficient escaping from a local minimum by molecular dynamics simulations,[56−58] or finding transition states[84] in which artificial constraints have been used for avoiding useless efforts.

When one starts from an arbitrary point on the scaled hypersphere surface, a minimum point can easily be reached by geometry optimization. The dent around this minimum can be removed by an elimination procedure using a suitable cosine shape function as in section II.B. Iterative treatments in this manner will be continued to find a number of minima on the hypersphere until all of them are eliminated. Mathematically, minima surrounded by circular series of "mountains" higher than the reference harmonic potential cannot be found in the above algorithm, when the optimization starts from the outside region. However, in chemical systems repulsive potential energies higher than the reference harmonic potential value are highly unlikely to surround the reaction path completely in all the $2(f - 1)$ directions. It follows that this iterative optimization−elimination technique may be expected to yield all minima on the hypersphere for chemical systems.

In practice, optimization processes of energy-minimization on the scaled hypersurface are at first made independently starting from $2f$ points at intersections with the normal coordinate directions. A set of independent minima found in the initial step are treated by the peak-fitting technique with cosine function, as in the case of section II.B. Elimination of found minima on the scaled hypersphere is then made with cosine shape functions. IOE treatments are made for the scaled hypersphere with renewed values until no minima are found. To make the decision to terminate the IOE procedure, we used an algorithm, where a 0 or 1 index was attached for each $2f$ starting points in our programs. Initially, all indexes for $2f$ starting points are set to be 0. If energy minimization starting from ith point succeeds to locate downward minima, the index for the ith point remained 0. If a minimum located by energy minimization starting from the jth point is judged to be a false path according to the criterion mentioned in section II.B, the index for the jth point was changed to 1. Finally, the IOE procedure is terminated if all indexes for $2f$ starting points become 1. In this procedure, $n + 2f$ times energy minimizations are required for obtaining n downward minima, where $2f$ times extra energy minimizations are required to confirm whether other minima exist or not.

D. Algorithm. Here, we describe the entire algorithm for global mapping of ab initio PES by use of the SHS method in combination with downhill walking algorithms. In procedures of global mapping, all energy, gradient, and Hessian evaluations and geometry optimizations were made by use of GAUSSIAN03 programs.[85]

(1) The geometry is optimized to obtain the starting EQ point.

(2) Normal-mode analysis takes place at the starting EQ point.

(3) An initial search for SHS paths is done by the IOE technique.

In the SHS procedures, the reference harmonic energy $''\epsilon$ for the scaled hypersphere surface (the energy value $''\epsilon$ of the isoenergy harmonic hypersphere surface) needed to be chosen suitably for the smallest sphere, since values that are too small may overlook the minima and hidden minima. The radius r of the hypersphere in the scaled coordinates is related to the energy ϵ by an equation $''\epsilon = (1/2)r^2$ or $r = (2\epsilon)^{1/2}$. We found that the harmonic vibrational quantum ϵ_S for the softest mode, estimated by the normal coordinate analysis at the starting EQ, is suitable, and we used a hypersphere corresponding to $\epsilon = \epsilon_S$ for the initial search by the IOE technique.

(4) Uphill walking is done along SHS paths.

Once SHS paths were obtained by the IOE technique, we can efficiently follow SHS paths by use of the predictor−corrector procedure. The current position of the SHS paths can simply be projected onto the new hypersphere, and then from the projected points, optimization procedures can be started. In the course of energy minimizations on hypersurfaces, a point **q** was optimized in polar coordinate representations of multidimensional PES as are used in our polar coordinate representation of PES.[86] The RFO method, including size-independent modification,[87] was used for energy minimization on the scaled hypersphere surface. First and second derivatives of energy as functions of polar coordinate angles were numerically calculated on second-order PES expanded using gradient and Hessian evaluations in the Cartesian coordinate. The Hessian matrix was calculated at the first iteration of the SHS path point optimization on the smallest hypersphere, and then it was updated by use of the method proposed by Farkas and Schlegel,[87] which include the hybrid use of Broyden−Fletcher−Goldfarb−Shanno[88] and Murtagh−Sargent[89] updated matrixes combined with the square root of the Bofill's constant.[90] With every 20 iterations of SHS path point optimization, an exact Hessian matrix was calculated to obtain efficient path following, because CPU time for the Hessian calculation is only 2 or 3 times longer than the force evaluation in the present cases of ab initio calculations.

The successive sizes of the hyperspheres to continue the SHS procedures were taken to be $r = n\epsilon^{1/2}$ with $n = 1, 2, 3, ...$, and $\epsilon = \epsilon_S$, corresponding to one quantum for the softest mode, was used for uphill walking. The SHS procedures were continued until the pathways reach TS/DC or they were found to be false pathways as mentioned above. Since the gradient vector is usually pointing at an exiting direction from the basin of the starting EQ, the pathway was judged to pass over the top of a SHS path if the gradient vector reversely directs at the starting EQ. To estimate the top of the SHS path, each interval of successive SHS path points were linearly interpolated, and the energy curve along the SHS path was fitted by the cubic spline method using functions of path lengths. Then, the top of the SHS path was estimated at the energy maximum on the SHS path. The RFO[27] method implemented in the GAUSSIAN03 programs[85] was used for refining TS structures from the top of the SHS path. When the nearest interatomic distance between two fragments became larger than 3 Å, the corresponding pathway was considered a DC.

(5) Downhill walking goes on along the steepest descent path.

To find a new EQ, downhill walking along the steepest descent path is done starting from the SHS path points judged to pass over the top of the SHS path. The second-order method using gradients and Hessian[75] calculations was used to follow the steepest descent paths.

(6) The global mapping continues by returning to procedure 2 to start from another EQ point if there are EQ that have not been used as a starting point for SHS procedures.

(7) The global mapping is terminated.

III. Results and Discussion

A. Formaldehyde. There are many theoretical investigations concerning the PES of the formaldehyde molecule.[91−99] In connection with photodissociation reactions yielding carbon monoxide and hydrogen molecules ($HCHO \rightarrow CO + H_2$) or HCO radical and hydrogen atom ($HCHO \rightarrow HCO + H$),[100−107] development of analytical PES[108−113] and dynamical simulations[109−112,114,115] of these reactions has been done extensively. In 1996, the first systematic global analysis of the ab initio HF/STO-3G surface was made by Bondensgård and Jensen,[44] and they found four EQ (omitting dissociated structures) and eight TS by the GEF aproach. Quapp et al.[46] also undertook global analysis of the surface by use of their RGF method and reported some more structures that were not reported by Bondensgård and Jensen.

In this study, we applied the present SHS method to the PES described by the B3LYP/6-31G level of theory. EQ and TS obtained on the PES were refined by the B3LYP/6-311++G(d,p) level of theory using structures on the B3LYP/6-31G surface as initial guesses for geometry optimizations. IRC calculations starting from each TS on the B3LYP/6-311++G(d,p) surface were also done to confirm the connection between each EQ. There is no dramatic changes between the topology of 6-31G and 6-311++G(d,p) surfaces in this study, and there are minor changes in some geometrical parameters. Zero-point vibration energy (ZPE) values on the B3LYP/6-311++G(d,p) surface were estimated with a scaling factor of 0.96. Finally, energy values at optimized structures on the B3LYP/6-311++G(d,p) surface were calculated by the CCSD(T)/cc-pVTZ level of theory (this series of calculations is denoted as the CCSD(T)/cc-pVTZ//B3LYP/6-311++G(d,p) level).

Figure 3 shows obtained topology of the present CCSD(T)/cc-pVTZ//B3LYP/6-311++G(d,p) level calculation. TS between EQ*n* and EQ*m* are labeled as TS*n*/*m*, and TS for dissociation channels from EQ*n* are labeled as TS*n*/D. Relative energy (including ZPE corrections) values toward formaldehyde molecule (EQ1) are also shown in Figure 3. Table 1 lists relative energy values toward EQ1 by various levels of theory used in this study. The energy barrier for the reaction (formaldehyde $\rightarrow H_2 + CO$) was estimated to be 82.0 kcal/mol by the CCSD(T)/cc-pVTZ//B3LYP/6-311++G(d,p) level. The value is almost the same as the best estimate (81.9±0.3 kcal/mol) based on the single reference theory by Feller et al.,[97] though it is slightly higher than the experimental value (79.2 ± 0.8 kcal/mol)[103] of Stark level crossing spectroscopy and value calculated by the multireference (12,11)-MRMP/cc-pVQZ level of theory (79.1 kcal/mol).[95] The topology of the part including EQ1−3 is almost the same as Hartree−Fock surfaces reported by Jensen et al.[44,96] and Quapp et al.[46] without a very high energy (more than 150 kcal/mol) area of PES. However, the part including EQ4,5 is clearly different from previously reported Hartree−Fock surfaces.[44,46,96] There is an additional EQ5 on the present B3LYP surface between EQ4 and the dissociation channel via TS5/D, though EQ4 is reported to dissociate directly into carbon monoxide and hydrogen molecules via similar TS to TS5/D.[46,96] Planar EQ5 has a pair of asymmetric OH bonds with their bond length of 0.969 and 1.757 Å. Although EQ5 can also be located as very shallow minima on PES by MP2/cc-pVTZ level of theory (EQ5 is 7.5 kcal/mol more stable than EQ4 on this surface), it may be an artifact of the employed B3LYP method, since EQ5 is just a bond stretch isomer of EQ4.

Here, we discuss TS that could not be obtained by the SHS method, even though they exist on B3LYP/6-31G surface. Jensen et al.[44,96] and Quapp et al.[46] reported TS2/2 (Figure 4(a, overlooked TS)) for the hydrogen exchange reaction of EQ2, and TS3/Db (Figure 4b, overlooked TS) for the dissociation reaction. These TS also exist on the B3LYP/6-31G surface, and Figure 4 shows structures on the B3LYP/6-31G surface. We can explain the reason that the SHS method could not locate these structures as follows. As described in section II.B, downward distortions reading toward TS or DC should overlap on the scaled hypersphere surface if they are placed on a competing direction, and these overlapped distortions were

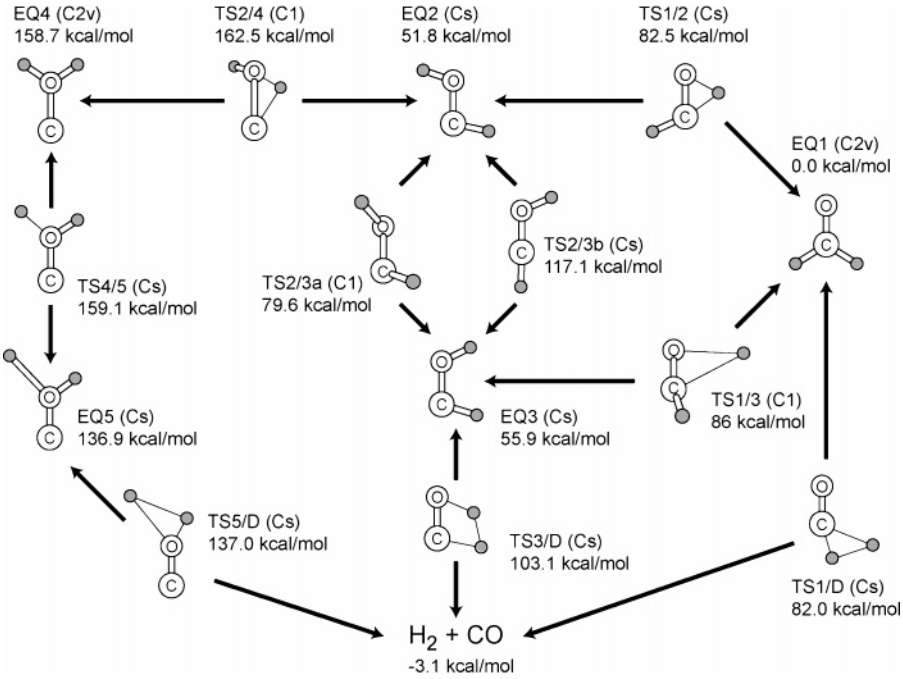

Figure 3. Topology of the PES for formaldehyde molecule obtained by the present CCSD(T)/cc-pVTZ//B3LYP/6-311++G(d,p) level calculation. TS between EQ*n* and EQ*m* are labeled as TS*n*/*m*, and TS for dissociation channels from EQ*n* are labeled as TS*n*/D. Relative energy (including zero point energy corrections) values (kcal/mol) toward formaldehyde molecule (EQ1) are also shown. For each structure, double solid lines denote chemical bonds, and thin single lines indicate a set of bonds rearranging at the TS.

TABLE 1: Energy (kcal/mol) of Five EQ Points and Nine TS Points Obtained by Application of the SHS Method to the Potential Energy Surface of Formaldehyde Molecule

	B3LYP[a]	B3LYP[a] + ZPE[b]	CCSD(T)[c]	CCSD(T)[c] + ZPE[b]	ZPE[b]
EQ1	0.0	0	0	0	16.0
EQ2	52.5	52.6	51.7	51.8	16.1
EQ3	58.3	57.8	56.3	55.9	15.5
EQ4	159.4	156.7	161.4	158.7	13.3
EQ5	157.3	152.6	141.6	136.9	11.2
TS1/D	84.9	80.1	86.8	82.0	11.2
TS1/2	87.1	83.4	86.1	82.5	12.3
TS1/3	125.4	119.2	92.4	86.2	9.8
TS2/3a	82.4	79.9	82.1	79.6	13.4
TS2/3b	113.7	111.7	119.1	117.1	14.0
TS2/4	168.5	164.7	166.3	162.5	12.2
TS3/D	111.1	105.5	108.7	103.1	10.3
TS4/5	161.0	156.3	163.8	159.1	11.2
TS5/D	160.9	154.6	143.3	137.0	9.7

[a] B3LYP/6-311++G(d,p) energy calculated at geometry optimized by the same level of theory. [b] Zero-point energy (ZPE) with a scaling factor of 0.96 calculated at the B3LYP/6-311++G(d,p) level of theory. [c] CCSD(T)/cc-pVTZ energy calculated at geometry optimized at the B3LYP/6-311++G(d,p) level of theory (CCSD(T)/cc-pVTZ//B3LYP/6-311++G(d,p)).

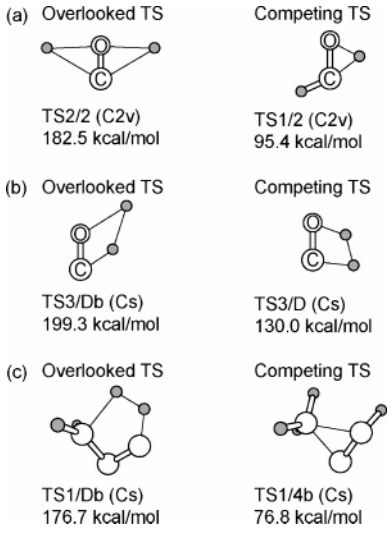

Figure 4. TS overlooked by the SHS method (overlooked TS) and TS for competing reactions (competing TS). Their relative energy values (kcal/mol) toward EQ1 (formaldehyde molecule for a and b, propyne molecule for c) calculated on the surface where the SHS method was applied (B3LYP/6-31G for formaldehyde, HF/6-31G for propyne).

separated by fitting them with cosine functions in this study. However, the very simple technique could not detect overly small distortion if covered by a very large distortion. Figure 4 lists TS overlooked by the SHS method (overlooked TS) and TS for competing reactions (competing TS) (see section III.B about Figure 4c). Their relative energy values toward EQ1 calculated on the surface where the SHS method was applied (B3LYP/6-31G surface in formaldehyde case) are also presented in Figure 4. The overlooked path toward TS2/2 from EQ2 is competing with the path toward TS1/2, since the H atom bonded to the O atom of EQ2 moves toward the C atom side in both reactions. Downward distortions corresponding to these reactions are placed on the same part of the scaled hypersphere surface and are interfering with each other. Here, the barrier height of TS2/2 is extremely higher than that of TS1/2, so the very small downward minimum on the scaled hypersphere surface corresponding to the reaction via TS2/2 was hidden by a fitting error of a relatively larger downward minimum corresponding to the reaction via TS1/2. The overlooked path toward TS3/Db from EQ3 is also competing with the path toward TS3/D, since the reactant and product of these reactions are the same. The barrier height of TS3/Db is extremely higher than that of TS3/D, so a very small downward minimum on the scaled hypersphere surface corresponding to the reaction via TS3/Db was hidden by a fitting error of a larger downward minimum corresponding to the reaction via TS3/D. Although overlapped downward distortions may become clearly separated as individual minima

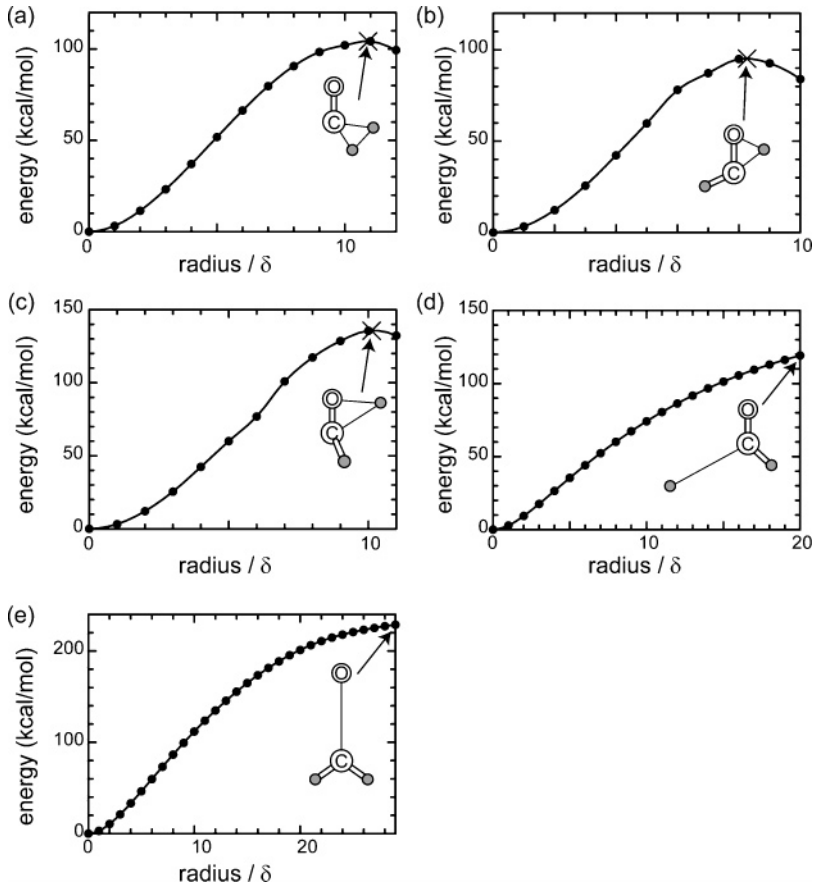

Figure 5. Energy profiles (kcal/mol) along SHS paths of (a) EQ1 → H_2 + CO, (b) EQ1 → EQ2, (c) EQ1 → EQ3, (d) EQ1 → HCO + H, and (e) EQ1 → CH_2 + O reactions. Parts a−c also show structures of the estimated top of SHS paths (see section II.D about these estimations). The radius r (δ) indicates sizes of successive hyperspheres used in the SHS procedures and are taken to be $r = n\epsilon^{1/2} = n\delta$ with $n = 1, 2, 3, ...$, and $\epsilon = \epsilon_S$, corresponding to one quantum for the softest mode (the softest mode of EQ1 is the out-of-plane bending motion with respective vibrational quantum $\epsilon_S = 1203.1$ cm^{-1} on the B3LYP/6-31G surface).

as the hypersphere radii increase, some extra ab initio calculations are required to detect their separation on the path following the predictor−corrector procedure as described in section II.D.4. More accurate fitting of downward minima with additional ab initio calculations may also overcome the problem; however, the two overlooked reactions are almost useless in the topology of the formaldehyde PES with extremely high activation barriers in comparison with competing reactions in Figure 4.

By the IOE procedures around the starting EQ1, 13 SHS paths were detected as downward minima on the scaled hypersphere surface. One of them was estimated to be a false path and vanished at the second step of the path following procedure (see section II.B about judging a false path). Although six of the remaining 12 paths can be omitted if the C_{2v} symmetry of EQ1 was considered, we did not use symmetries in the present procedures. Figure 5 shows energy profiles along SHS paths of (a) EQ1 → H_2 + CO, (b) EQ1 → EQ2, (c) EQ1 → EQ3, (d) EQ1 → HCO + H, and (e) EQ1 → CH_2 + O reactions. Figure 5a−c also shows structures of the estimated top of the SHS paths (see section II.D about these estimations). SHS paths in these cases (Figure 5a−c) passed through nearby TS, and geometry optimizations using the top of the SHS paths as an initial guess easily converged to the corresponding TS. Two of these (Figure 5d,e) are direct dissociation channels, and one more symmetrically independent path corresponds to a false path. Since the false path was produced by a fitting error of the downward minima corresponding to the reaction EQ1 → H_2 + CO of Figure 5a, its walk also reached to the top of the SHS path and finally decomposed into H_2 + CO, though geometry optimization from the top of the SHS path failed to converge to any stationary point. Table 2 shows the SHS path connections between each EQ of Figure 3. The number of connections, *i*, indicates there are *i* SHS path connections starting from the corresponding EQ*n* of the first column toward EQ*m* (or dissociation into H_2 + CO) of the first line. The SHS path connections shown in Table 2 are very simple and very similar to IRC connections shown in Figure 3, though there are two more SHS path connections than IRC. Although the employed wave function in this study cannot quantitatively describe radical dissociations such as the path shown in Figure 5d, there were some other SHS paths corresponding to such processes yielding H + CHO, H + COH, or CH + OH.

TABLE 2: Connection of SHS Paths on the B3LYP/6-31G Potential Energy Surface of Formaldehyde Molecule[a]

	EQ1	EQ2	EQ3	EQ4	EQ5	H_2 + CO
EQ1		1	1			1
EQ2	1		2	1		
EQ3	1	2			1[b]	1
EQ4		1	1		1	
EQ5		1[c]		1		1

[a] The first column shows the starting EQ points. Number of connection *i* indicates that there are *i* SHS path connections starting from the corresponding EQ*n* of the first column toward EQ*m* (or dissociation into H_2 + CO) of the first line. [b] There is no IRC connection between EQ3 and EQ5, and final TS optimization starting from the top of SHS path converge to TS2/4. [c] There is no IRC connection between EQ5 and EQ2, and the final TS optimization starting from the top of the SHS path did not converge to any stationary point.

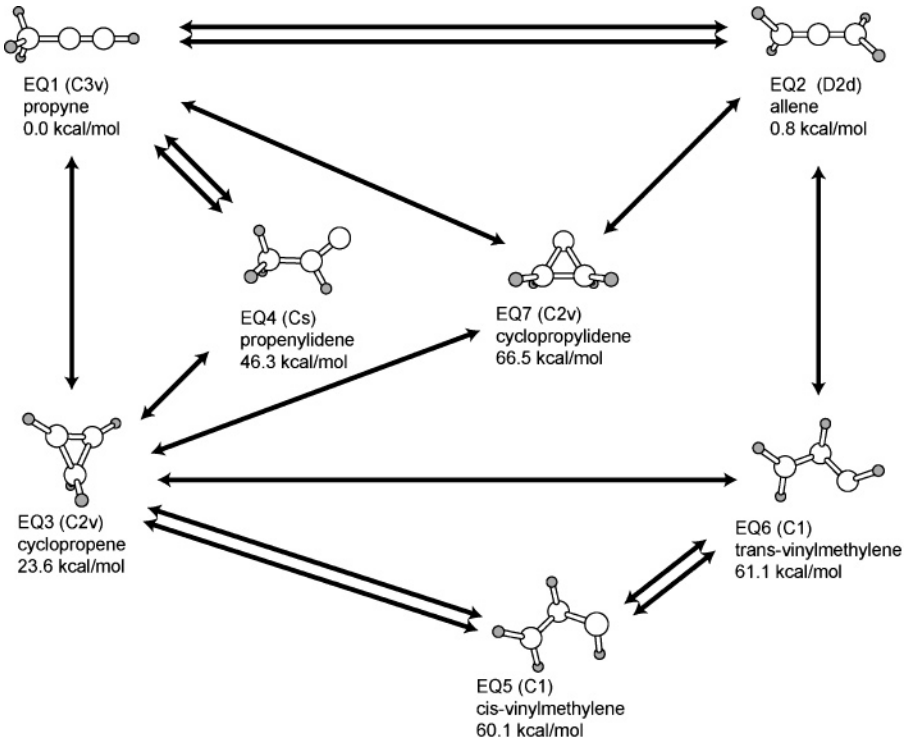

Figure 6. Connections between obtained EQ on the PES for propyne molecule of the present CCSD(T)/cc-pVTZ//B3LYP/6-311++G(d,p) level of calculations. An arrow indicates an independent IRC connection between a pair of pointed EQs. Relative energy (including zero-point energy corrections) values (kcal/mol) toward propyne molecule (EQ1) are also shown.

The final behavior of the false paths produced by the fitting error of the downward minima can be classified into the next three patterns:

(1) vanishing because of the criterion of section II.B;

(2) joining into the true DC path corresponding to the downward minima producing the false path, when the cosine faction corresponding to the DC path was removed because of the criterion to reach DC (see section II.D about the judging criterion of DC); and

(3) entering into a new potential well by walking around the true SHS path corresponding to the downward minimum producing the false path.

In the case of pattern 3, though one cannot judge whether the path is a false path or a true SHS path, there is no problem in practical global mapping procedures because the false path also finds a new potential well by walking around the corresponding true SHS path. Furthermore, there is no diverging and wandering behavior in false path walking, since false paths arising from fitting error of true SHS paths should walk around corresponding true SHS paths.

The number of SHS paths produced in the present global mapping was only 58. The number of paths arising from all-mode-following procedure starting from all 14 stationary points becomes 168. Since the GEF and RGF methods also use higher order stationary points as starting points, Bondensgård and Jensen followed 336 GEF paths starting from 28 stationary points,[44] and Quapp et al. followed 588 REF paths starting from 49 stationary points.[46] From the simplicity of path connection network and the number of paths, the present SHS method can be considered to be much more efficient than these all-mode-following techniques.

B. Propyne. The propyne molecule and its stable isomers (allene and cyclopropene) are known to be very important intermediates in combustion processes, and their isomerization and dissociation reactions have been investigated very extensively by both experiment[116−127] and theoretical calculations.[7,8,121,122,124−126,128−139] Photodissociation experiments of a propyne molecule have been reported,[140−147] and theoretical calculations considering both ground and excited-state reactions have also been made.[148,149] Although many of these calculations are concerned with some limited parts of PES for analyzing particular reactions, Miller and Klippensteine recently obtained a global picture of the PES for their multiwell master equation analyses by geometry optimizations at the B3LYP/6-311++G(d,p) level and one-point energy at their original high-level model calculations.[8]

In this study, we applied the present SHS method to PES described by the HF/6-31G level of theory. EQ and TS obtained on the PES were refined by the B3LYP/6-311++G(d,p) level of theory by using structures on the HF/6-31G surface as initial guesses for geometry optimizations. IRC calculations starting from each TS on the B3LYP/6-311++G(d,p) surface was also made to confirm the connection between each EQ. Zero-point vibration energy (ZPE) values on the B3LYP/6-311++G(d,p) surface were estimated with a scaling factor of 0.96. Finally, energy values at optimized structures on B3LYP/6-311++G(d,p) surface were calculated by the CCSD(T)/cc-pVTZ level of theory. Figure 6 shows connections between the obtained EQ of the present CCSD(T)/cc-pVTZ//B3LYP/6-311++G(d,p) level of calculations, and each arrow indicates an independent IRC connection between a pair of pointed EQs. Figure 7 shows the TS obtained for the CCSD(T)/cc-pVTZ//B3LYP/6-311++G(d,p) level of calculations. TS between EQ*n* and EQ*m* are labeled as TS*n*/*m* or TS*n*/*m*a, TS*n*/*m*b, ..., if there are multiple connections between EQ*n* and EQ*m*. TS for dissociation channels from EQ*n* are labeled as TS*n*/D, or TS*n*/Da, TS*n*/Db, ..., if there are multiple connections. Relative energy (including ZPE corrections) values toward the propyne molecule (EQ1) are also shown in Figures 6 and 7. Table 3 lists relative energy values toward EQ1 by various levels of theory used in this study. Although 12 EQ and 43 TS were obtained on the HF/6-31G surface, five EQ corresponding to

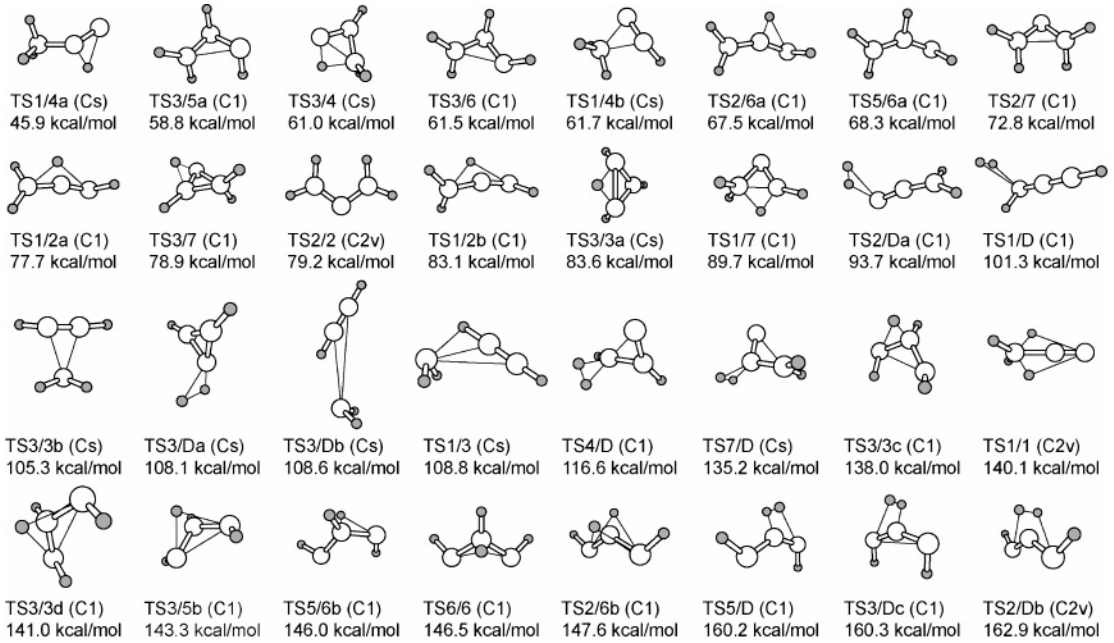

Figure 7. TS obtained by the CCSD(T)/cc-pVTZ//B3LYP/6-311++G(d,p) level of calculations. TS between EQ*n* and EQ*m* are labeled as TS*n*/*m*, or TS*n*/*m*a, TS*n*/*m*b, ..., if there are multiple connections between EQ*n* and EQ*m*. TS for dissociation channels from EQ*n* are labeled as TS*n*/D, or TS*n*/Da, TS*n*/Db, ..., if there are multiple connections. Relative energy (including zero-point energy corrections) values (kcal/mol) toward propyne molecule (EQ1) are also shown. For each structure, double solid lines denote chemical bonds, and thin single lines indicate a set of bonds rearranging at TS.

1,3-propanediylidene ($CHCH_2CH$) isomers could not be obtained as potential minima on the B3LYP/6-311++G(d,p) surface. In another seven EQ, there are minor changes between HF/6-31G and B3LYP/6-311++G(d,p) in some geometrical parameters. Although vinylmethylene species corresponding to EQ5 and EQ6 in Figure 6 were located as very shallow local minima on both HF and B3LYP surfaces based on restricted wave function, their most stable structure is known to be a triplet-state allylic structure[128,130,135] and is also reported to have large spin contamination on the singlet B3LYP surface based on unrestricted wave function.[8] In connection with vanished $CHCH_2CH$ isomers, many TS for isomerization reactions between them also vanished, though some TS for dissociation reactions from them remained as very high energy dissociation channels from lower energy EQ (TS2/Db, TS3/Dc, and TS5/D). The number of EQ obtained in this study is the same as results that Miller and Klippensteine obtained by B3LYP/6-311++G(d,p) calculations based on unrestricted wave function.[8] However, they reported nine TS in their calculations,[8] while we obtained 32 TS by the first systematic exploration of the PES. There are many TS connecting equivalent structures (TS1/1, TS2/2a,b, TS3/3a−d, and TS6/6); for example, TS1/1 is corresponding to the synchronous hydrogen exchange reaction in propyne molecule reported also for methanol molecule.[17] Many very high energy TS were also newly obtained (TS2/Db, TS3/5b, TS3/Dc, TS5/6b, and TS5/D). Since the heat of formations of propyne (EQ1) by radical reaction ($CH_2CCH + H \rightarrow$ propyne) and cyclopropene (EQ3) by collision between singlet methylene and acetylene ($CH_2 + HCCH \rightarrow$ cyclopropene) are both ca. 90 kcal/mol, an important energy range for this system may become up to ca. 110 kcal/mol. Although the two-step reaction via TS1/4a and TS3/4 was previously known as the route between EQ1 and EQ3, there is direct connection via TS1/3 between them. The direct connection between EQ1 and EQ7 via TS1/7 was also newly located, and there are new H_2 dissociation channels from EQ4 and EQ7. Although TS3/Db is corresponding to the dissociation path yielding acetylene and singlet methylene, the TS connects EQ3 with a weakly bound van der Waals type complex of dissociated species, and then the overall reaction between infinitely separated acetylene and singlet methylene is barrierless.

Here, we discuss some other TS reported previously. Yoshimine et al. presented a route connecting EQ1 with EQ6 directly on the MCSCF/4-31G surface.[131] Although a similar TS for the same connection was also obtained by the SHS method on the HF/6-31G surface, geometry optimization starting from the structure converged to TS1/2a on the B3LYP/6-311++G(d,p) surface. They also reported a route between EQ2 and EQ5 on the MCSCF/4-31G saface,[131] and geometry optimization starting from the structure reported in their paper converged to TS2/6 on both HF/6-31G and B3LYP/6-311++G(d,p) surfaces. Walch[134] and Guadagnini et al.[136] obtained two pathways directly connecting EQ1 with EQ3 via a TS similar to vinylmethylene (EQ5 and EQ6) of this study. On the CASSCF/pVDZ surface explored by their calculations, since all EQ without *cis*-vinylmethylene (EQ5) were reported to exist, the very shallow well of EQ5 on the B3LYP/6-311++G(d,p) surface may correspond to the TS region on the CASSCF/pVDZ surface. These changes around vinylmethylene (very shallow wells of EQ5 and EQ6) are problems of the level of theory for energy calculations, and then they are not problems of the SHS method. However, the SHS method could not find the TS1/Db[8,149] shown in Figure 4c, even though this exists on both the HF/6-31G and B3LYP/6-311++G(d,p) surfaces. The reason the SHS method could not find this can also be explained by the fitting error of downward minima, as discussed in section III.A. Figure 4 lists TS overlooked by the SHS method and TS for competing reactions (see Section III.A for discussion about Figure 4a,b). Their relative energy values toward EQ1 calculated on the surface where the SHS method was applied (HF/6-31G surface in propyne case) are also presented in Figure 4. Since both TS1/Db and TS1/4b arise by movement along the CCC bending motion of EQ1, downward minima corresponding to their SHS paths are placed on the same part of the scaled hypersphere surface and are interfering. Here, TS1/Db energy is extremely higher than TS1/4b energy on the

TABLE 3: Energy (kcal/mol) of Seven EQ Points and 32 TS Points Obtained by Application of the SHS Method to the Potential Energy Surface of Propyne Molecule

	B3LYP[a]	B3LYP[a] + ZPE[b]	CCSD(T)[c]	CCSD(T)[c] + ZPE[b]	ZPE[b]
EQ1	0.0	0	0	0	33.4
EQ2	−1.6	−2.0	1.2	0.8	33.0
EQ3	24.2	24.3	23.5	23.6	33.6
EQ4	47.8	46.2	47.9	46.3	31.8
EQ5	60.8	59.6	61.3	60.1	32.2
EQ6	60.6	59.3	62.5	61.1	32.1
EQ7	68.3	66.8	68.0	66.5	31.9
TS1/4a	47.8	45.8	47.8	45.9	31.5
TS3/5a	61.0	59.4	60.4	58.8	31.9
TS3/4	64.9	62.4	63.4	61.0	31.0
TS3/6	61.2	59.6	63.1	61.5	31.9
TS1/4b	64.0	62.4	63.4	61.7	31.7
TS2/6a	67.2	64.0	70.8	67.5	30.2
TS5/6a	68.3	65.3	71.4	68.3	30.4
TS2/7	73.2	71.4	74.5	72.8	31.7
TS1/2a	81.0	77.0	81.7	77.7	29.5
TS3/7	82.6	80.2	81.3	78.9	31.0
TS2/2	74.6	76.3	77.6	79.2	35.1
TS1/2b	83.5	79.7	86.9	83.1	29.6
TS3/3a	86.4	82.5	87.5	83.6	29.5
TS1/7	93.1	90.1	92.7	89.7	30.4
TS2/Da	95.3	88.7	100.4	93.7	26.8
TS1/D	102.9	95.4	108.9	101.3	25.9
TS3/3b	109.9	105.9	109.3	105.3	29.4
TS3/Da	111.9	106.0	114.0	108.1	27.5
TS3/Db	116.4	110.2	114.8	108.6	27.3
TS1/3	114.2	108.9	114.0	108.8	28.2
TS4/D	118.6	113.6	121.6	116.6	28.5
TS7/D	138.5	132.0	141.6	135.2	26.9
TS3/3c	141.1	136.7	142.3	138.0	29.1
TS1/1	144.4	139.5	145.1	140.1	28.5
TS3/3d	144.6	140.5	145.1	141.0	29.3
TS3/5b	146.7	142.1	147.9	143.3	28.8
TS5/6b	151.3	145.7	151.6	146.0	27.8
TS6/6	151.8	146.6	151.7	146.5	28.3
TS2/6b	153.2	147.8	153.0	147.6	28.0
TS5/D	162.4	155.8	166.8	160.2	26.8
TS3/Dc	161.7	155.4	166.6	160.3	27.1
TS2/Db	166.2	159.1	170.0	162.9	26.3

[a] B3LYP/6-311++G(d,p) energy calculated at geometry optimized by the same level of theory. [b] Zero-point energy (ZPE) with a scaling factor of 0.96 calculated at the B3LYP/6-311++G(d,p) level of theory. [c] CCSD(T)/cc-pVTZ energy calculated at geometry optimized at the B3LYP/6-311++G(d,p) level of theory (CCSD(T)/cc-pVTZ//B3LYP/6-311++G(d,p)).

HF/6-31G surface, as shown in Figure 4c, and thus very small downward minima on the scaled hypersphere surface corresponding to the reaction via TS1/Db was hidden by a fitting error of the large downward minima corresponding to the reaction via TS1/4b.

Although many new reactions are newly obtained, there is no dramatic change in the lowest barrier connections between seven isomers. However, it should be noted that the global picture of this PES, which was constructed by extensive theoretical calculations[7,8,121,122,124−126,128−139,148,149] over two decades, could be obtained by a single systematic global analysis by the SHS method.

IV. Concluding remarks

We descried technical details for application of the recently proposed scaled hypersphere search method[67] to ab initio PES. We also reported applications of the SHS method to formaldehyde and propyne molecules and obtained new global picture of their PES. Connections of SHS paths between each EQ are very similar to corresponding IRC connections, as shown in previous applications toward two-dimensional model potentials[67] and also shown in present application to formaldehyde (see Table 2). The energy maximum along the SHS path is similar to the corresponding TS,[67,68] and geometry optimizations from the structure easily converged to TS. The present applications of the SHS method located five EQ and nine TS on the PES for formaldehyde molecule and seven EQ and 32 TS on the PES for propyne molecule.

Global analyses by use of the SHS method are efficient in comparison with other mode-following techniques. The number of SHS paths discovered for formaldehyde and propyne molecules are 58 and 421, respectively. Here, following all $(3N - 6)$-mode for an N-atom system, starting from all 14 and 55 stationary points obtained on the surface where the SHS method was applied (B3LYP/6-31G for formaldehyde, HF/6-31G for propyne), yields 168 and 1650 paths for formaldehyde and propyne molecules, respectively. The present SHS method selects searching directions by the SHS algorithm according to magnitude of anharmonicity, and thus it can avoid wandering around useless parts of the PES. The IOE technique for finding the initial part of SHS paths is very efficient and requires only $n + 2(3N - 6)$ times energy minimization calculations on the scaled hypersphere surface for obtaining n SHS paths. Here, $2(3N - 6)$ extra energy minimizations are needed to confirm that there are no more SHS paths on the hypersphere. Since topology on the small-sized scaled hypersphere is very simple (completely flat if the PES is harmonic), demands of the IOE procedure were smaller than the cost of walking up toward the energy maximum of one SHS path in the present applications. We previously demonstrated a very accurate interpolation technique for ab initio PES by use of the simplicity of topology on the scaled hypersphere surface, where a PES was constructed by successive cubic spline fitting of anharmonic distortions on several sizes of scaled hypersphere surfaces.[86] The higher energy part of PES is rather complicated, and furthermore, SCF convergence may become slower, and thus it may be too late to decide whether TS exist in the chosen mode direction or not after climbing up to and wandering around the higher energy region. It should be more efficient to select walking directions on a very simple small-sized scaled hypersphere surface.

Of course, the present SHS method is not mathematically confirmed to obtain all EQ and all TS, as in the same for any other surface-walking approach. As described for two examples of the present applications, there is the possibility of overlooking very shallow downward minima (corresponding to reactions via extremely high energy TS) in the IOE procedure if there are some deeper downward minima placed on the same part of the scaled hypersphere surface. Although the problem may be overcome by developing an accurate fitting technique for larger downward minimum, that should require extra costs for ab initio calculations in the fitting procedures. Since overlapped downward minima become clearly separated individual minima as the hypersphere radii increase, an algorithm that detects separations of the path being followed may also solve the problem with some extra ab initio calculations. However, the three overlooked TS have extremely higher activation barriers than other competing reaction paths (see Figure 4), and thus this problem is not important for obtaining a chemically useful topology of the PES by the SHS method. The SHS method does not work if the reaction path is rounding from the radial direction to the tangential direction, though it may not occur on the PES for chemical reactions. As already mentioned in connection with Figures 1 and 2, the present SHS method is based on chemical intuition concerning anharmonic downward distortion of the PES

associated with potential crossing or dissociation where long-range attractive interactions are operative. Transition state properties have been studied for reaction potentials around the reactant or the product in many theoretical treatments of chemical reactions. The Bell, Evans, and Polanyi principle;[4,62] the Hammond postulate;[63] frontier molecular orbital theory;[59,60] and the Marcus equation[61] also assume that the potentials of the reactant and the product are closely related with the activation energy and the location of the TS. Thus, the present SHS algorithm is expected to be applicable to many chemical systems in which the relationship between EQ and TS is straightforward.

Acknowledgment. The present work was supported partly by a Grant-in-Aid for Scientific Research from the Japanese Ministry of Education, Culture, Sports, Science and Technology. S.M. is supported by the Research Fellowship of the Japan Society for the Promotion of Science for Young Scientists.

References and Notes

(1) Schlegel, H. B. *J. Comput. Chem.* **2003**, *24*, 1514.
(2) Fukui, K. *Acc. Chem. Res.* **1981**, *14*, 363.
(3) Eyring, H. *J. Chem. Phys.* **1934**, *3*, 107.
(4) Evans, M. G.; Polanyi, M. *J. Chem. Soc., Faraday Trans.* **1936**, *32*, 1340.
(5) Truhlar, D. G.; Garret, B. C.; Klippenstein, S. J. *J. Phys. Chem.* **1996**, *100*, 12771.
(6) Oref, I.; Tardy, D. C. *Chem. Rev.* **1990**, *90*, 1407.
(7) Frankcombe, T. J.; Smith, S. C. *J. Chem. Phys.* **2003**, *119*, 12729.
(8) Miller, J. A.; Klippenstein, S. J. *J. Phys. Chem. A* **2003**, *107*, 2680.
(9) Ischtwan, J.; Collins, M. A. *J. Chem. Phys.* **1994**, *100*, 8080.
(10) Collins, M. A. *Theor. Chem. Acc.* **2002**, *108*, 313.
(11) Moyano, G. E.; Collins, M. A. *J. Chem. Phys.* **2004**, *121*, 9769.
(12) Fukuzawa, K.; Osamura, Y. *Astrophys. J.* **1997**, *489*, 113.
(13) Basiuk, V. A. *J. Phys. Chem. A* **2001**, *105*, 4252.
(14) Ding, Y. H.; Li, Z. S.; Huang, X. R.; Sun, C. C. *J. Phys. Chem. A* **2001**, *105*, 5896.
(15) Wang, J. H.; Han, K. L.; He, G. Z.; Li, Z.; Marris, V. R. *J. Phys. Chem. A* **2003**, *107*, 9825.
(16) Liu, H. L.; Huang, X. R.; Chen, G. H.; Ding, Y. H.; Sun, C. C. *J. Phys. Chem. A* **2004**, *108*, 6919.
(17) Osamura, Y.; Roberts, H.; Herbst, E. *Astron. Astrophys.* **2004**, *421*, 1101.
(18) McKee, M. L.; Wine, P. H. *J. Am. Chem. Soc.* **2001**, *123*, 2344.
(19) Zhu, R. S.; Lin, M. C. *J. Chem. Phys.* **2003**, *119*, 10667.
(20) Schnell, M.; Mühlhäuser, M.; Peyerimhoff, S. D. *J. Phys. Chem. A* **2004**, *108*, 1298.
(21) Petrie, S.; Osamura, Y. *J. Phys. Chem. A* **2004**, *108*, 3615.
(22) Petrie, S.; Osamura, Y. *J. Phys. Chem. A* **2004**, *108*, 3623.
(23) Howorth, N. L.; Mackie, J. C.; Bacskay, G. B. *J. Phys. Chem. A* **2003**, *107*, 6792.
(24) Tokmakov, I. V.; Lin, M. C. *J. Am. Chem. Soc.* **2003**, *125*, 11397.
(25) Andersen, A.; Carter, E. A. *J. Phys. Chem. A* **2003**, *107*, 9463.
(26) Westerberg, K. M.; Floudas, C. A. *J. Chem. Phys.* **1999**, *110*, 9259.
(27) Banerjee, A.; Adams, N.; Simons, J.; Shepard, R. *J. Phys. Chem.* **1985**, *89*, 52.
(28) Csaszar, P.; Pulay, P. *J. Mol. Struct.* **1984**, *114*, 31.
(29) Pancíø, J. *Collect. Czech. Chem. Commun.* **1974**, *40*, 1112.
(30) Cerjan, C. J.; Miller, W. H. *J. Chem. Phys.* **1981**, *75*, 2800.
(31) Simons, J.; Jørgensen, P.; Taylor, H.; Ozment, J. *J. Phys. Chem.* **1983**, *87*, 2745.
(32) Baker, J. *J. Comput. Chem.* **1986**, *7*, 385.
(33) Wales, D. J. *J. Chem. Phys.* **1994**, *101*, 3750.
(34) Munro, L. J.; Wales, D. J. *Phys. Rev. B* **1999**, *59*, 3969.
(35) Tsai, C. J.; Jordan, K. D. *J. Phys. Chem.* **1993**, *97*, 11227.
(36) Basilevsky, M. V.; Shamov, A. G. *Chem. Phys.* **1981**, *60*, 347.
(37) Basilevsky, M. V. *Chem. Phys.* **1982**, *67*, 337.
(38) Rowa, D. J.; Ryman, A. *J. Math. Phys.* **1982**, *23*, 732.
(39) Hoffman, D. K.; Nord, R. S.; Ruedenberg, K. *Theor. Chim. Acta* **1986**, *69*, 265.
(40) Jørgensen, P.; Jensen, H. J. A.; Helgaker, T. *Theor. Chim. Acta* **1988**, *73*, 55.
(41) Quapp, W. *Theor. Chim. Acta* **1989**, *75*, 447.
(42) Schlegel, H. B. *Theor. Chim. Acta* **1992**, *83*, 15.
(43) Sun, J.-Q.; Ruedenberg, K. *J. Chem. Phys.* **1993**, *98*, 9707.
(44) Bondensgård, K.; Jensen, F. *J. Chem. Phys.* **1996**, *104*, 8025.
(45) Jensen, F. *Introduction to Computational Chemistry;* Wiley: Chichester, 1998.
(46) Quapp, W.; Hirsch, M.; Imig, O.; Heidrich, D. *J. Comput. Chem.* **1998**, *19*, 1087.
(47) Quapp, W.; Hirsch, M.; Heidrich, D. *Theor. Chem. Acc.* **1998**, *100*, 285.
(48) Bofill, J. M.; Anglada, J. M. *Theor. Chem. Acc.* **2001**, *105*, 463.
(49) Crehuet, R.; Bofill, J. M.; Anglada, J. M. *Theor. Chem. Acc.* **2002**, *107*, 130.
(50) Hirsch, M.; Quapp, W. *J. Comput. Chem.* **2002**, *23*, 887.
(51) Dallos, M.; Lischka, H.; Monte, E. V. D.; Hirsch, M.; Quapp, W. *J. Comput. Chem.* **2002**, *23*, 576.
(52) Barkema, G. T.; Mousseau, N. *Phys. Rev. Lett.* **1996**, *77*, 4358.
(53) Mousseau, N.; Barkema, G. T. *Phys. Rev. E* **1998**, *57*, 2419.
(54) Doye, J. P. K.; Miller, M. A.; Wales, D. J. *J. Chem. Phys.* **1999**, *110*, 6896.
(55) Wales, D. J.; Doye, J. P. K.; Miller, M. A.; Mortenson, P. N.; Walsh, T. R. *Adv. Chem. Phys.* **2000**, *115*, 1.
(56) Laio, A.; Parrinello, M. *Proc. Natl. Acad. Sci. U.S.A.* **2002**, *99*, 12562.
(57) Martoòák, R.; Laio, A.; Parrinello, M. *Phys. Rev. Lett.* **2003**, *90*, 075503.
(58) Iannuzzi, M.; Laio, A.; Parrinello, M. *Phys. Rev. Lett.* **2003**, *90*, 238302.
(59) Fukui, K.; Yonezawa, T.; Shingu, H. *J. Chem. Phys.* **1952**, *20*, 722.
(60) Fleming, I. *Frontier Orbitals and Organic Chemical Reactions*; Wiley: London, 1976.
(61) Marcus, R. A. *J. Phys. Chem.* **1968**, *72*, 891.
(62) Bell, R. P. *Proc. R. Soc. London, Ser. A* **1936**, *154*, 414.
(63) Hammond, G. S. *J. Am. Chem. Soc.* **1955**, *77*, 334.
(64) Jensen, F. *J. Am. Chem. Soc.* **1992**, *114*, 1596.
(65) Ruedenberg, K.; Sun, J.-Q. *J. Chem. Phys.* **1994**, *101*, 2168.
(66) Olsen, P. T.; Jensen, F. *J. Chem. Phys.* **2003**, *118*, 3523.
(67) Ohno, K.; Maeda, S. *Chem. Phys. Lett.* **2004**, *384*, 277.
(68) Maeda, S.; Ohno, K. *Chem. Phys. Lett.* **2005**, *404*, 95.
(69) Maeda, S.; Ohno, K. *Chem. Lett.* **2004**, *33*, 1372.
(70) Maeda, S.; Ohno, K. *Chem. Phys. Lett.* **2004**, *398*, 240.
(71) Ishida, K.; Morokuma, K.; Komornicki, A. *J. Chem. Phys.* **1977**, *66*, 2153.
(72) Müller, K.; Brown, L. D. *Theor. Chim. Acta* **1979**, *53*, 75.
(73) Schmidt, M. W.; Gordon, M. S.; Dupuis, M. *J. Am. Chem. Soc.* **1985**, *107*, 2585.
(74) Garrett, B. C.; Redmon, M. J.; Steckler, R.; Truhlar, D. G.; Baldridge, K. K.; Bartol, D.; Schidt, M. W.; Gordon, M. S. *J. Phys. Chem.* **1988**, *92*, 1476.
(75) Page, M.; McIver, J. W., Jr. *J. Chem. Phys.* **1988**, *88*, 922.
(76) Gonzalez, C.; Schlegel, H. B. *J. Chem. Phys.* **1989**, *90*, 2154.
(77) Gonzalez, C.; Schlegel, H. B. *J. Chem. Phys.* **1991**, *95*, 5853.
(78) Sun, J.-Q.; Ruedenberg, K. *J. Chem. Phys.* **1993**, *99*, 5269.
(79) Hratchian, H. P.; Schlegel, H. B. *J. Chem. Phys.* **2004**, *120*, 9918.
(80) Dewar, M. J. S.; Healy, E. F.; Stewart, J. J. P. *J. Chem. Soc., Faraday Trans. 2* **1984**, *80*, 227.
(81) Abashkin, Y.; Russo, N. *J. Chem. Phys.* **1994**, *100*, 4477.
(82) Pillardy J.; Piela, L. *J. Phys. Chem.* **1995**, *99*, 11805.
(83) Wawak, R. J.; Pillardy, J.; Liwo, A.; Gibson, K. D.; Scheraga, H. A. *J. Phys. Chem. A* **1998**, *102*, 2904.
(84) Peters, B.; Liang, W.; Bell, A. T.; Chakraborty, A. *J. Chem. Phys.* **2003**, *118*, 9533.
(85) Frisch, M. J.; Trucks, G. W.; Schlegel, H. B.; Scuseria, G. E.; Robb, M. A.; Cheeseman, J. R.; Montgomery, J. A., Jr.; Vreven, T.; Kudin, K. N.; Burant, J. C.; Millam, J. M.; Iyengar, S. S.; Tomasi, J.; Barone, V.; Mennucci, B.; Cossi, M.; Scalmani, G.; Rega, N.; Petersson, G. A.; Nakatsuji, H.; Hada, M.; Ehara, M.; Toyota, K.; Fukuda, R.; Hasegawa, J.; Ishida, M.; Nakajima, T.; Honda, Y.; Kitao, O.; Nakai, H.; Klene, M.; Li, X.; Knox, J. E.; Hratchian, H. P.; Cross, J. B.; Adamo, C.; Jaramillo, J.; Gomperts, R.; Stratmann, R. E.; Yazyev, O.; Austin, A. J.; Cammi, R.; Pomelli, C.; Ochterski, J. W.; Ayala, P. Y.; Morokuma, K.; Voth, G. A.; Salvador, P.; Dannenberg, J. J.; Zakrzewski, V. G.; Dapprich, S.; Daniels, A. D.; Strain, M. C.; Farkas, O.; Malick, D. K.; Rabuck, A. D.; Raghavachari, K.; Foresman, J. B.; Ortiz, J. V.; Cui, Q.; Baboul, A. G.; Clifford, S.; Cioslowski, J.; Stefanov, B. B.; Liu, G.; Liashenko, A.; Piskorz, P.; Komaromi, I.; Martin, R. L.; Fox, D. J.; Keith, T.; Al-Laham, M. A.; Peng, C. Y.; Nanayakkara, A.; Challacombe, M.; Gill, P. M. W.; Johnson, B.; Chen, W.; Wong, M. W.; Gonzalez, C.; Pople, J. A. *GAUSSIAN03, Revision C.02*; Gaussian, Inc., Wallingford, CT, 2004.
(86) Maeda, S.; Ohno, K. *Chem. Phys. Lett.* **2003**, *381*, 177.
(87) Farkas, Ö.; Schlegel, H. B. *J. Chem. Phys.* **1999**, *111*, 10806.
(88) Broyden, C. G. *J. Inst. Math. Appl.* **1970**, *6*, 76. Fletcher, R. *Comput. J. (Switzerland)* **1970**, *13*, 317. Goldfarb, D. *Math. Comput.* **1970**, *24*, 23. Shanno, D. F. *ibid.* **1970**, *24*, 647.
(89) Murtagh, B.; Sargent, R. W. H. *Comput. J. (Switzerland)* **1972**, *13*, 185.
(90) Bofill, J. M. *J. Comput. Chem.* **1994**, *15*, 1.

(91) Goddard, J. D.; Schaefer, H. F., III *J. Chem. Phys.* **1979**, *70*, 5117.
(92) Pople, J. A.; Raghavachari, K.; Frisch, M. J.; Binkley, J. S.; Schleyer, P. v. R. *J. Am. Chem. Soc.* **1983**, *105*, 6389.
(93) Scuseria, G. E.; Schaefer, H. F., III *J. Chem. Phys.* **1989**, *90*, 3629.
(94) Deng, L.; Ziegler, T.; Fan, L. *J. Chem. Phys.* **1993**, *99*, 3823.
(95) Nakano, H.; Nakayama, K.; Hirao, K.; Dupuis, M. *J. Chem. Phys.* **1997**, *106*, 4912.
(96) Jensen, F. *Theor. Chem. Acc.* **1998**, *99*, 295.
(97) Feller, D.; Dupuis, M.; Garrett, B. C. *J. Chem. Phys.* **2000**, *113*, 218.
(98) Bauerfeldt, G. F.; de Albuquerque, L. M. M.; Arbilla, G.; da Silva, E. C. *Theochem* **2002**, *580*, 147.
(99) Jalbout, A. F.; Chang, C. M. *Theochem* **2003**, *634*, 127.
(100) Clouthier, D. J.; Ramsey, D. A. *Annu. Rev. Phys. Chem.* **1983**, *34*, 31.
(101) Moore, C. B.; Weisshaar, J. C. *Annu. Rev. Phys. Chem.* **1983**, *34*, 525.
(102) Guyer, D. R.; Polik, W. F.; Moore, C. B. *J. Chem. Phys.* **1986**, *84*, 6519.
(103) Polik, W. F.; Guyer, D. R.; Moore, C. B. *J. Chem. Phys.* **1990**, *92*, 3453.
(104) Green, W. H., Jr.; Moore, C. B.; Polik, W. F. *Annu. Rev. Phys. Chem.* **1992**, *43*, 591.
(105) van Zee, R. D.; Foltz, M. F.; Moore, C. B. *J. Chem. Phys.* **1993**, *99*, 1664.
(106) Terentis, A. C.; Waugh, S. E.; Metha, G. F.; Kable, S. H. *J. Chem. Phys.* **1998**, *108*, 3187.
(107) Valachovic, L. R.; Tuchler, M. F.; Dulligan, M.; Droz-Georget, Th.; Zyrianov, M.; Kolessov, A.; Reisler, H.; Wittig, C. *J. Chem. Phys.* **2000**, *112*, 2752.
(108) Carter, S.; Mills, I. M.; Murrell, J. N. *Mol. Phys.* **1980**, *39*, 455.
(109) Farantos, S. C.; Murrell, J. N. *Mol. Phys.* **1980**, *40*, 883.
(110) Chang, Y.-T.; Minichino, C.; Miller, W. H. *J. Chem. Phys.* **1992**, *96*, 4341.
(111) Sung, B. J.; Kim, M. S. *J. Chem. Phys.* **2000**, *113*, 3098.
(112) Yonehara, T.; Kato, S. *J. Chem. Phys.* **2002**, *117*, 11131.
(113) Zhang, X.; Zou, S.; Harding, L. B.; Bowman, J. M. *J. Phys. Chem. A* **2004**, *108*, 8980.
(114) Li, X.; Millam, J. M.; Schlegel, H. B. *J. Chem. Phys.* **2000**, *113*, 10062.
(115) Schlegel, H. B.; Iyengar, S. S.; Li, X.; Millam, J. M.; Voth, G. A.; Scuseria, G. E.; Frisch, M. J. *J. Chem. Phys.* **2002**, *117*, 8694.
(116) Bradley, J. N.; West, K. O. *J. Chem. Soc., Faraday Trans. 1* **1975**, *71*, 967.
(117) Lifshitz, A.; Frenklach, M.; Burcat, A. *J. Phys. Chem.* **1975**, *79*, 1148.
(118) Walsh, R. *J. Chem. Soc., Faraday Trans. 1* **1976**, *72*, 2137.
(119) Bailey, I. M.; Walsh, R. *J. Chem. Soc., Faraday Trans. 1* **1978**, *74*, 1146.
(120) Hopf, H.; Priebe, H.; Walsh, R. *J. Am. Chem. Soc.* **1980**, *102*, 1210.
(121) Kakumoto, T.; Ushirogouchi, T.; Saito, K.; Imamura, A. *J. Phys. Chem.* **1987**, *91*, 183.
(122) Karni, M.; Oref, I.; Barzilai-Gilboa, S.; Lifshitz, A. *J. Phys. Chem.* **1988**, *92*, 6924.
(123) Adamson, J. D.; Morter, C. L.; DeSain, J. D.; Glass, G. P.; Curl, R. F. *J. Phys. Chem.* **1996**, *100*, 2125.
(124) Kiefer, J. H.; Mudipalli, P. S.; Sidhu, S. S.; Kern, R. D.; Jursic, B. S.; Xie, K.; Chen, H. *J. Phys. Chem. A* **1997**, *101*, 4057.
(125) Davis, S. G.; Law, C. K.; Wang, H. *J. Phys. Chem. A* **1999**, *103*, 5889.
(126) Blitz, M. A.; Beasley, M. S.; Pilling, M. J.; Robertson, S. H. *Phys. Chem. Chem. Phys.* **2000**, *2*, 805.
(127) Davis, H. F.; Shu, J.; Peterka, D. S.; Ahmed, M. *J. Chem. Phys.* **2004**, *121*, 6254.
(128) Honjou, N.; Pacansky, J.; Yoshimine, M. *J. Am. Chem. Soc.* **1984**, *106*, 5361.
(129) Honjou, N.; Pacansky, J.; Yoshimine, M. *J. Am. Chem. Soc.* **1985**, *107*, 5332.
(130) Yoshimine, M.; Pacansky, J.; Honjou, N. *J. Am. Chem. Soc.* **1989**, *111*, 2785.
(131) Yoshimine, M.; Pacansky, J.; Honjou, N. *J. Am. Chem. Soc.* **1989**, *111*, 4198.
(132) Bauschlicher, C. W., Jr.; Langhoff, S. R. *Chem. Phys. Lett.* **1992**, *193*, 380.
(133) Kiefer, J. H.; Kumaran, S. S.; Mudipalli, P. S. *Chem. Phys. Lett.* **1994**, *224*, 51.
(134) Walch, S. P. *J. Chem. Phys.* **1995**, *103*, 7064.
(135) Kakkar, R.; Padhi, B. S. *Int. J. Quantum. Chem.* **1996**, *58*, 389.
(136) Guadagnini, R.; Schatz, G. C.; Walch, S. P. *J. Phys. Chem. A* **1998**, *102*, 5857.
(137) Frankcombe, T. J.; Smith, S. C.; Gates, K. E.; Robertson, S. H. *Phys. Chem. Chem. Phys.* **2000**, *2*, 793.
(138) Frankcombe, T. J.; Smith, S. C. *Faraday Discuss.* **2001**, *119*, 159.
(139) Yu, H.-G.; Muckerman, J. T. *J. Phys. Chem. A* **2005**, *109*, 1890.
(140) Jackson, W. M.; Anex, D. S.; Continetti, R. E.; Lee, Y. T. *J. Phys. Chem.* **1991**, *95*, 7327.
(141) Satyapal, S.; Bersohn, R. *J. Phys. Chem.* **1991**, *95*, 8004.
(142) Seki, K.; Okabe, H. *J. Phys. Chem.* **1992**, *96*, 3345.
(143) Song, X.; Bao, Y.; Urdahl, R. S.; Gosine, J. N.; Jackson, W. M. *Chem. Phys. Lett.* **1994**, *217*, 216.
(144) Ni, C.-K.; Huang, J. D.; Chen, Y. T.; Kung, A. H.; Jackson, W. M. *J. Chem. Phys.* **1999**, *110*, 3320.
(145) Sun, W.; Yokoyama, K.; Robinson, J. C.; Suits, A. G.; Neumark, D. M. *J. Chem. Phys.* **1999**, *110*, 4363.
(146) Harich, S.; Lin, J. J.; Lee, Y. T.; Yang, X. *J. Chem. Phys.* **2000**, *112*, 6656.
(147) Qadiri, R. H.; Feltham, E. J.; Nahler, N. H.; García, R. P.; Ashfold, M. N. R. *J. Chem. Phys.* **2003**, *119*, 12842.
(148) Jackson, W. M.; Mebel, A. M.; Lin, S. H.; Lee, Y. T. *J. Phys. Chem. A* **1997**, *101*, 6638.
(149) Mebel, A. M.; Jackson, W. M.; Chang, A. H. H.; Lin, S. H. *J. Am. Chem. Soc.* **1998**, *120*, 5751.